THE JOURNAL OF BIOLOGICAL CHEMISTRY VOL. 285, NO. 18, pp. 13357–13363, April 30, 2010


# The C Terminus of SipC Binds and Bundles F-actin to Promote *Salmonella* Invasion[S]

Received for publication, December 11, 2009, and in revised form, February 9, 2010 Published, JBC Papers in Press, March 8, 2010, DOI 10.1074/jbc.M109.094045

**Sebenzile K. Myeni and Daoguo Zhou**[1]

*From the Department of Biological Sciences, Purdue University, West Lafayette, Indiana 47907*

***Salmonella enterica serovar* Typhimurium invade non-phagocytic cells by injecting bacterial effector proteins to exploit the host actin cytoskeleton network. SipC is such a *Salmonella* effector known to nucleate actin, bundle F-actin, and translocate type III effectors. The molecular mechanism of how SipC bundles F-actin and SipC domains responsible for these activities are not well characterized. We successfully separated these activities through a series of genetic deletion/insertions in SipC. We found that the C terminus (amino acids 200–409) of SipC bundled actin filaments using *in vitro* biochemical assays. We further demonstrated that amino acid residues 221–260 and 381–409 of full-length SipC were indispensable for its actin binding and bundling activities. Furthermore, *Salmonella* mutant strains lacking the actin bundling activity were less invasive into HeLa cells. These studies indicate that the C terminus of SipC bundles F-actin to promote *Salmonella* invasion.**

*Salmonella enterica* serovar typhimurium (*S. typhimurium*) are Gram-negative enteropathogenic bacteria that infect a variety of mammalian, avian, and reptile hosts and are responsible for a range of illness in humans including gastroenteritis and typhoid fever. These diseases are among the most common food-borne diseases in humans and represent a major public health and economical burden worldwide (1–6). *Salmonella* species have evolved sophisticated virulence mechanisms to manipulate host cell functions to their own benefit. These include specialized type III protein secretion systems (TTSSs) capable of translocating a panel of bacterial effectors directly into the host cell (3, 7). Some of these effectors engage and manipulate the host actin cytoskeleton machinery to facilitate bacterial internalization into host cells (3, 7–11). The translocation of these effectors through the host plasma membrane requires *Salmonella* SipB, SipC, and SipD (12–16).

Many actin-binding proteins use a set of structural modules to achieve diverse activities and generate distinct topologies of F-actin bundles (17). F-actin-bundling proteins generally exert their actin bundling activities by encoding two discrete actin binding domains within their sequence or by forming a multimeric complex that bridges two F-actin filaments together into a bundle. For example, plastin (Fimbrin) has two actin binding domains in close proximity to tightly bundle F-actin in microvilli (18). Furthermore, proteins like $\alpha$-actinin form homodimers in an antiparallel manner to produce more loosely ordered F-actin structures such as stress fibers (19). Moreover, villin uses one of its actin binding sites and bundles F-actin filaments via dimerization (20).

A number of type III effector proteins possess multiple functions (7). SipC is a multifunctional protein known to nucleate and bundle actin in addition to its type III effector translocation activity. We have previously separated SipC nucleation activity from its effector translocation activity and demonstrated that its actin nucleation activity plays a key role in *Salmonella*-induced actin cytoskeleton rearrangements and bacterial invasion (21). The molecular mechanism and the domain by which SipC bundles F-actin remain unclear. Here, we separated the actin bundling activity from its nucleation activity. We present evidence that the C terminus of SipC bundles F-actin and contributes to *Salmonella* invasion.

## MATERIALS AND METHODS

*Bacterial Strains and Infection*—Wild-type *S. typhimurium* strain SL1344 and its *sipC* (SB220)-null mutant have been previously described (12, 13, 22). Chromosomal gene replacements were carried out by using a suicide plasmid as previously described (21, 23). *Salmonella* infection of mammalian cells was carried out as previously described (8) at a multiplicity of infection (moi) of 10 for 15 min. The ability of bacteria to invade host cell was evaluated using the inside/outside differential staining assay as previously described (21) at least three times (with >500 cells counted each time). Statistical analysis was performed using Student's *t* test and GraphPad Prism 5 software. The mammalian cell line HeLa (CCL-2) was purchased from the ATCC cell biology stock center (Manassas, VA) and was maintained in Dulbecco's modified Eagle's medium supplemented with 10% fetal bovine serum.

*Protein Purification*—His-tagged recombinant SipC protein and its derivatives were expressed and purified in *Escherichia coli* BL21 (DE3) using the pET expression system (EMD Biosciences, Madison, WI). The purification of the His-tagged proteins was performed under denaturing conditions according to the manufacturer's instructions (Invitrogen, Carlsbad, CA) with slight modifications as described previously (21). His-tagged T-plastin was expressed in *E. coli* and purified under native conditions following similar procedures. Actin was isolated from rabbit skeletal muscle as described by (24) and further purified by Sephadex G-200 chromatography in G-buffer (5 mM Tris-HCl at pH 8.0, 0.1 mM $CaCl_2$, 0.2 mM ATP, 1 mM dithiothreitol, and 0.01% $NaN_3$). Purified proteins were concentrated and buffer exchanged in 100 mM NaCl, 20 mM Tris-HCl, pH 8.0, using a 10,000 and 30,000 molecular weight cut-off

[S] The on-line version of this article (available at http://www.jbc.org) contains supplemental Figs. S1 and S2.

[1] To whom correspondence should be addressed. Tel.: 765-494-8159; Fax: 765-494-0876; E-mail: zhoud@purdue.edu.

dialysis cassette (Sartorius, Elk Grove, IL). Purified proteins were snap-frozen in liquid nitrogen and stored at −80 °C. Proteins were preclarified at 120,000 × *g*, and their concentration was determined by Bradford assay (Bio-Rad) using bovine serum albumin as standard.

*Actin Assays*—Actin nucleation assays were performed using pyrene-labeled actin in G-buffer (2 mM Tris-HCl, pH 7.5, 0.2 mM dithiothreitol, 0.2 mM $CaCl_2$) as previously described (21). Fluorescence intensity was measured on a fluorescence spectrophotometer (Fluoromax-3, Jobin Yvon, Edison, NJ) with the excitation wavelength set at 365 nm, and the emission wavelength at 405 nm. Polymerization was initiated by adding actin polymerization buffer from a 50× stock solution (100 mM $MgCl_2$, 2.5 M KCl). F-actin cross-linking or bundling assays were carried out using the low-speed co-sedimentation assays as previously described (25). Briefly, monomeric rabbit G-actin was polymerized at room temperature in F-actin buffer (5 mM Tris-HCl at pH 7.8, 0.2 mM ATP, 1 mM dithiothreitol, 0.1 mM $CaCl_2$, 1 mM $MgCl_2$, and 100 mM KCl) for 1 h and preclarified at low-speed (10,000 × *g*). Purified recombinant proteins were preclarified at 120,000 × *g* for 30 min and subsequently incubated with F-actin for 60 min at room temperature. The mixture was then centrifuged for 30 min at 10,000 × *g* in a microcentrifuge at 4 °C. Equal amounts of starting materials, supernatants, and pellets were resolved on an SDS-PAGE gel and visualized with Coomassie Brilliant Blue R-250 (EMD, Gibbstown, NJ) staining. The amount of proteins was quantified densitometrically (Image Quant 5.1, Molecular Dynamics) and was expressed as percentages of actin in the pellet. Each assay was repeated at least five times with similar results. The presence of actin bundles was also visualized by fluorescence microscopy as previously reported (26). F-actin was mixed with varying concentrations of recombinant proteins in F-buffer and incubated at room temperature for 30 min. F-actin was then labeled with rhodamine-phalloidin with 0.1% DABCO and 0.1% methylcellulose. Samples were mounted on coverslips coated with poly-lysine and visualized with a Zeiss AxioVert 200M deconvolution microscope. For the *in vitro* G-actin and F-actin binding assays, purified recombinant proteins were desalted with protein desalting spin columns (Pierce) and further dialyzed against G-buffer. All recombinant proteins and G-actin were preclarified at 120,000 × *g* for 1 h before pull-down assays were performed. G-actin or freshly polymerized F-actin at final concentration of 4 μM was incubated with 4 μM of purified proteins and incubated at 4 °C for 2 h. Purified proteins were immobilized by adding Ni-nitrilotriacetic acid beads (Novagen, Gibbstown, NJ). Prior to adding beads, 20% of reactions were collected as inputs. The beads were then washed 5× in G-buffer containing 1% Nonidet P-40 for G-actin binding and F-buffer (with 1% Nonidet P-40) for F-actin binding. Pull-downs and inputs were re-suspended in SDS-PAGE sample buffer and subjected to SDS-PAGE and Western blot analysis using monoclonal anti-actin antibody (Sigma-Aldrich) and rabbit polyclonal anti-SipC antibody. For SipC-actin interaction *in vivo*, HEK293T cells were transfected with plasmids expressing SipC and its derivatives in pEGFP-N1. Transfected cells were lysed 48 h post-transfection in lysis buffer (20 mM Tris-HCl, pH 7.5, 150 mM NaCl, 1 mM EDTA, 1% Triton X-100, protease inhibitor cocktails, and 1 mM $Na_3VO_4$). The lysates were centrifuged at 15,000 × *g* for 15 min and precleared with TrueBlot anti-rabbit Ig IP Beads (eBioscience). The supernatants were then incubated with rabbit polyclonal GFP antibody overnight at 4 °C. TrueBlot anti-Rabbit Ig IP Beads were added and further incubated for 1 h at 4 °C. The immune complex was separated by SDS-PAGE, and proteins detected by Western blot using the TrueBlot protocol (eBioscience).

*Electron Microscopy*—Actin filaments and bundles were formed as described above for the low-speed co-sedimentation assays except diluted 10 times with F-buffer before mounting on the mesh grids. The mixture was applied onto a 400 carbon-coated nickel mesh grid and allowed to adhere to the carbon film for a few seconds, followed by staining with 2% uranyl acetate. Samples were imaged using a Philips CM-100 transmission electron microscope operated at 80 kV, 200 μm condenser aperture, 50 μm objective aperture, and spot 3. Images were captured on Kodak SO-163 film.

## RESULTS

*The C Terminus of SipC Mediates F-actin Bundling*—Previous studies have shown that the C-terminal amino acid region (amino acids 200–409, SipC-C)[2] is required for its actin nucleation activity (21, 27, 28). During the characterization of SipC-mediated actin nucleation activity by fluorescent and electron microscopy, we noticed abundant F-actin bundles when SipC-C was present together with F-actin filaments. Because the F-actin bundling activity of SipC was previously reported to be conferred only by the N terminus (amino acids 1–120, SipC-N) (28), we decided to examine the bundling activity of SipC in more detail.

We first sought to determine whether SipC-N or SipC-C confers the F-actin bundling activity of SipC. Full-length SipC, truncated SipC-N, and SipC-C were purified as previously described (Fig. 1*A*) (27, 28). A quantitative low-speed co-sedimentation assay was employed to measure the bundling activity of SipC and its derivatives. As expected, most F-actin remained in the supernatants when incubated alone. The majority of F-actin partitioned into the pellet fraction when T-plastin was added to the mixture (Fig. 1, *B* and *C*). When actin filaments were incubated in the presence of full-length SipC, SipC-C, more than 80% F-actin was precipitated into the pellet (Fig. 1, *B* and *C*). In contrast, less than 20% F-actin was found in the pellet in the presence of SipC-N (Fig. 1, *B* and *C*). We concluded that the C terminus of SipC (amino acids 200–409, SipC-C) mediates the F-actin bundling activity.

To further visualize the effect of SipC on F-actin bundling, we incubated F-actin and rhodamine-phalloidin with full-length SipC, SipC-N, or SipC-C. F-actin alone was used as a negative control, and T-plastin was added as a positive control. In the presence of full-length SipC or SipC-C, we observed F-actin cables similar to those induced by T-plastin (Fig. 1*D*) under the fluorescent microscope. In contrast, addition of SipC-N resulted in the F-actin appearance identical to that of

[2] The abbreviations used are: SipC-C, C terminus of SipC; SipC-N, N terminus of SipC; GFP, green fluorescent protein; EGFP, enhanced green fluorescent protein.

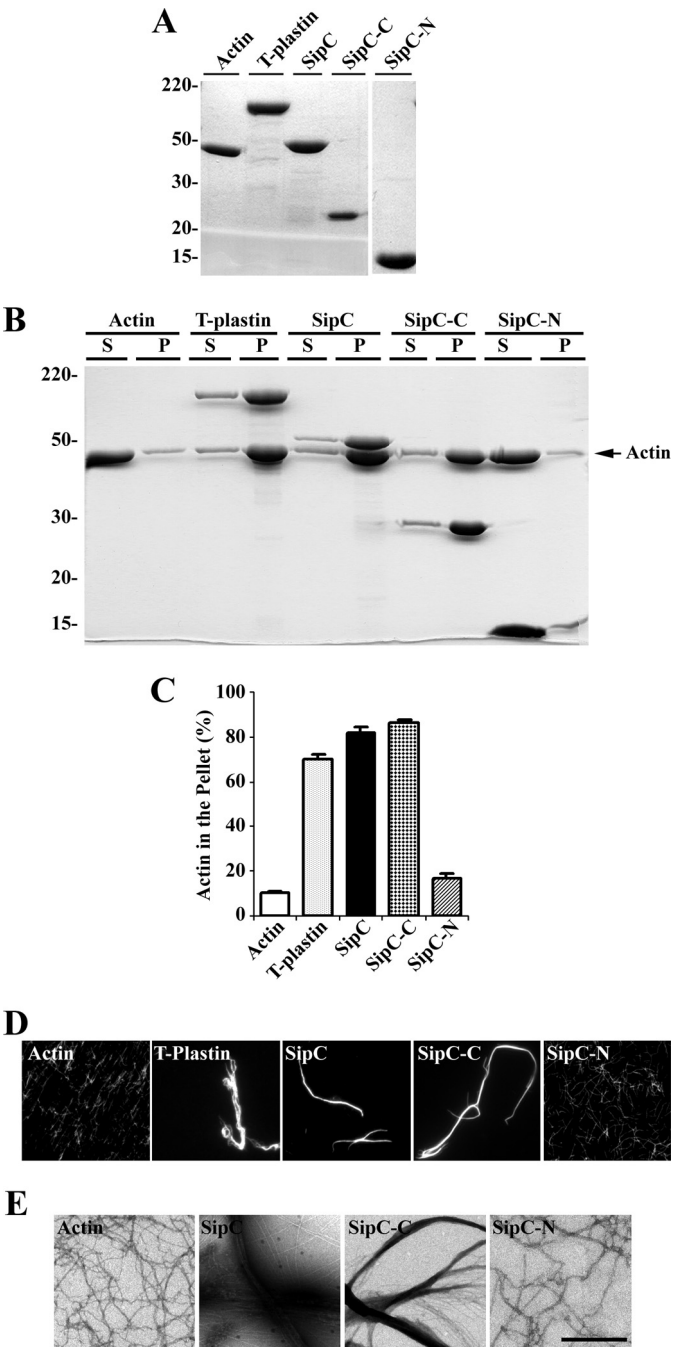


FIGURE 1. **The C terminus of SipC mediates F-actin bundling.** *A*, Coomassie staining of purified actin from rabbit skeletal muscle, recombinant T-plastin, full-length SipC, SipC-C, and SipC-N. The molecular masses of standard proteins are indicated on the *left* in kDa. *B*, F-actin bundling assay measured by the low speed co-sedimentation assay. F-actin was incubated alone, with T-plastin, full-length SipC, SipC-C, SipC-N proteins at room temperature, followed by centrifugation at 10,000 × *g* for 30 min. Supernatants and pellets were then resolved on an SDS-PAGE gel and visualized with Coomassie staining. *C*, quantification of F-actin bundling. The experiment in *C* was repeated five times, and the gels were scanned. The amount of actin present in the pellet and in the supernatant was quantified. F-actin bundling activity was expressed as the percentage of actin that sedimented in the total actin. Values represent means of five independent experiments with standard errors shown. *D*, F-actin bundles visualized by fluorescence microscopy. F-actin was incubated alone, with T-plastin, full-length SipC, the C terminus of SipC (SipC-C), or the N terminus of SipC (SipC-N) proteins at room temperature and subsequently labeled with rhodamine-phalloidin. *E*, F-actin bundles visualized by transmission election microscopy. F-actin was incubated alone, with full-length SipC, SipC-C, or SipC-N proteins.

F-actin alone (Fig. 1*D*). To eliminate the possibility that F-actin-binding phalloidin might play a role in F-actin bundling experiments above, we examined the effect of SipC, SipC-N, or SipC-C on F-actin bundling using electron microscopy. Consistent with the fluorescent microscopy data, full-length SipC, and SipC-C induced F-actin bundles, while F-actin incubated with SipC-N appeared to be similar to that of F-actin alone (Fig. 1*E*). These data suggest that SipC-C bundles F-actin.

*Distinct Domains Mediate F-actin Bundling and Actin Nucleation Activities*—SipC contains three putative domains: the N-terminal domain, the central hydrophobic region, and the C-terminal domain (28) (Fig. 2*A*). We previously constructed 10 in-frame deletion-insertion replacement mutations throughout the C-terminal domain of SipC (amino acids 201–409) (21). Each mutant contained a 20-residue deletion and the M45-tag (18 amino acids) epitope (29) was inserted at the deletion site (Fig. 2*A*, clones 1–10). Wild-type *sipC* gene with (clone 11) or without the M45 tag at the C termini was also made in a similar manner (21) (Fig. 2*A*).

To localize region(s) responsible for the actin bundling activity, we purified the C-terminal domain of SipC-C (amino acids 201–409) and its #1–11 derivatives as previously described. Purified recombinant proteins were then examined for their F-actin bundling activity by the low-speed co-sedimentation assay described above. SipC#2, SipC#3, and SipC#10 proteins exhibited reduced levels of F-actin bundling activity, while SipC#1 showed intermediate levels of activity (Fig. 2*B*). SipC#4, SipC#5, SipC#6, SipC#7, SipC#8, and SipC#9 mutant derivatives had similar levels of actin bundling activities comparable to that of the wild-type SipC-C (Fig. 2*B*).

Purified recombinant proteins were further examined for their F-actin bundling activity using rhodamine-phalloidin labeled F-actin. SipC#4, SipC#5, SipC#6, SipC#7, SipC#8, SipC#9 mutant derivatives induced F-actin cables similar to those induced by wild-type SipC-C and SipC-C#11 (Fig. 2*C*). In contrast, SipC#2, SipC#3, and SipC#10 lost their F-actin bundling activities (Fig. 2*C*). Similar results were observed by electron microscopy (Fig. 2*D*) as described above. SipC#1 showed intermediate levels of bundling under the electron microscope. To ensure that SipC#2, SipC#3, and SipC#10 proteins were functional, we measured their nucleation activities as previously reported (21). SipC#2, SipC#3, and SipC#10 proteins maintained their nucleation activity levels similar to that of wild-type SipC-C (supplemental Fig. S1). Taken together these data show that the amino acid residues 221–260 (SipC#2 and SipC#3) and 381–409 (SipC#10) of the C-terminal of SipC play a role in SipC-mediated F-actin bundling activity. Because the actin nucleation activity of SipC was previously mapped to amino acid residues 201–220 (SipC#1) (21), these data separate the F-actin bundling activity of SipC from its actin nucleation activity.

*The C-terminal End Region of SipC (amino acids 381–409) Binds F-actin and Is Essential for F-actin Bundling*—SipC has been shown to bundle and nucleate actin *in vitro*, although direct association and the SipC domains necessary for the interaction with actin have not been demonstrated. We therefore sought to map SipC regions involved in F-actin binding. Full-length SipC, truncated SipC-N and SipC-C were incubated

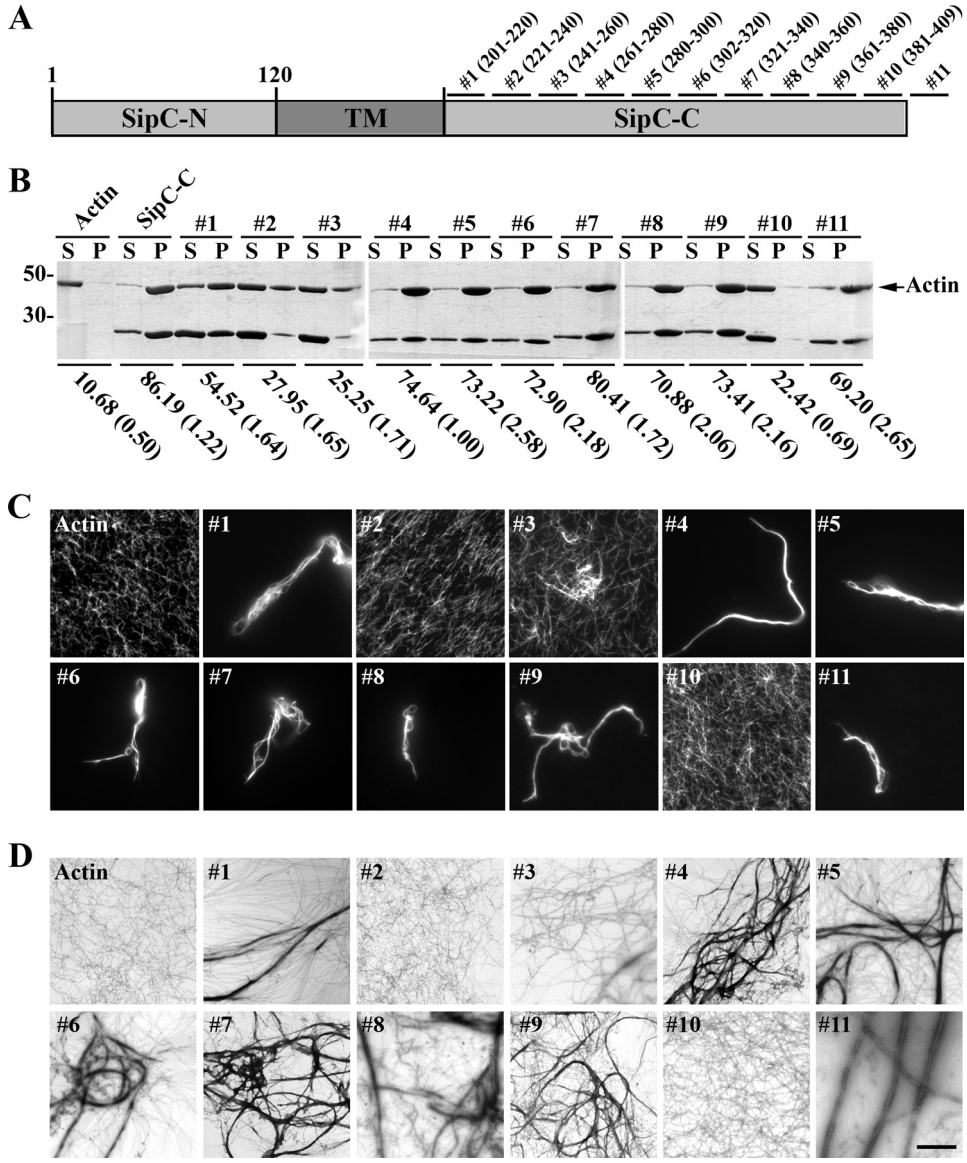


FIGURE 2. **The central (amino acids 221–260) and C-terminal (amino acids 381–409) regions of SipC-C are involved in F-actin bundling.** *A*, schematic diagram of wild-type SipC protein and its mutant derivative (1–11) proteins. SipC-N represents the N terminus amino acids 1–120, SipC-C represents the C-terminal amino acids 200–409, and TM represents the putative transmembrane region. *B*, F-actin bundling assay measured by the low speed co-sedimentation assay. F-actin was incubated alone, with SipC-C or its mutant derivatives at room temperature followed by centrifugation at 10,000 × *g* for 30 min. Supernatants and pellets were then resolved on an SDS-PAGE gel and visualized with Coomassie staining. The experiments were repeated five times and quantified by densitometry scanning. F-actin bundling activity was expressed as the percentage of actin that sediments in the total actin. Values represent means of five independent experiments with standard errors shown. F-actin bundles were visualized by fluorescence microscopy (*C*) and by transmission election microscopy (*D*). F-actin was incubated alone, with SipC-C mutant derivatives as described.

with F-actin, and their interaction was examined using pull-down assays. As shown in Fig, 3*A*, full-length SipC and SipC-C were able to interact with F-actin and SipC-N did not. Furthermore, wild-type SipC-C and most of its derivatives were able to bind F-actin. SipC-C#10 failed to bind F-actin while SipC-C#2 and -#3 had reduced binding to F-actin (Fig. 3*B*). Wild-type SipC-C and all its derivatives remain active in binding to G-actin as demonstrated by both the pull-down and by gel overlay assays (data not shown). SipC and SipC-C also bind to endogenous actin in tissue-cultured cells (Fig. 3*C*). Together, these results demonstrated that the tail region of SipC (amino acids 381–409) is essential for F-actin binding.

The above experiments were done using the truncated C-terminal domain of SipC-C (amino acids 201–409). We next asked whether amino acid residues 221–260 (#2 and #3) and 381–409 (#10) are required for the F-actin bundling activity of the full-length SipC. Similar #2, #3, and #10 mutations were introduced into the full-length SipC. Purified full-length SipC, SipC#2, SipC#3, and SipC#10 were then examined for their actin bundling activities *in vitro* by the low-speed co-sedimentation assay described above. Consistent with the data obtained with the truncated SipC-C, full-length SipC#2, SipC#3, and SipC#10 proteins failed to induce F-actin bundle formation while the full-length wild-type SipC was active in forming F-actin bundles (Fig. 4*A*). Similar results were obtained when their F-actin bundling activity was studied by electron microscopy (Fig. 4*B*). Furthermore, full-length SipC#2, SipC#3, and SipC#10 proteins had actin nucleation activity comparable to that of the wild-type SipC (data not shown). These data demonstrated that the C-terminal end region of SipC (amino acids 381–409) binds F-actin and two regions of SipC (amino acids 221–260 and 381–408) are essential for its F-actin bundling activity.

*SipC Mutants Deficient in F-actin Bundling Are Less Invasive into HeLa Cells*—To invade non-phagocytic cells, *Salmonella* secretes multiple effector proteins that engage the actin cytoskeleton to mediate bacterial entry (7). SipA, SipC, SopB, SopE, and SopE2 are all known to modulate host actin dynamics to promote *Salmonella* invasion. It is becoming evident that mutations in one effector often result in minor or even undetectable invasion defect using tissue-cultured cells. In fact, there was little detectable invasion defect when the F-actin bundling deficient mutants (*sipC*#2 and *sipC*#3) were examined in the wild-type background (data not shown). Mutations in *sipA*, or *sopB* result in a moderate reduction in *Salmonella* invasion while deletion of SopE led to a more dramatic decrease in invasion (8, 9, 11, 30). Because SipA and SopB may have an indirect role in actin bundling, we reasoned that the *sipAsopB* strain may eliminate/reduce functional redundancy. Thus, we decided to introduce the *sipC*#2 and *sipC*#3 mutations into the

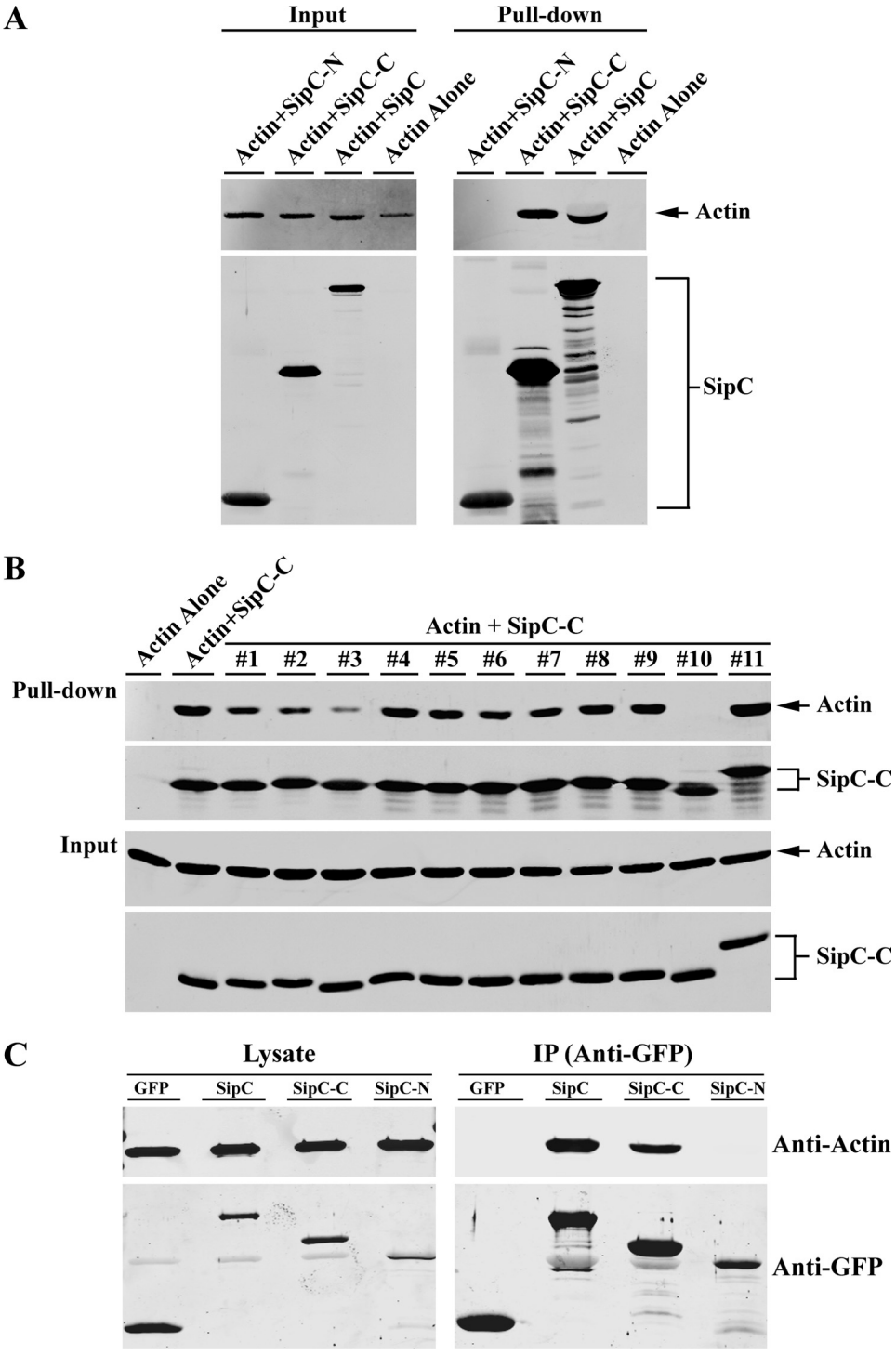


FIGURE 3. **The C-terminal end region of SipC (amino acids 381–409) binds F-actin.** Preformed F-actin was incubated alone or with full-length SipC, truncated SipC-N and SipC-C (*A*) or with SipC-C derivatives (*B*). SipC proteins were then pulled down by adding Ni-nitrilotriacetic acid beads. Pull-downs and inputs were separated by SDS-PAGE and actin was detected with anti-actin antibody, and SipC was visualized with polyclonal anti-SipC antibody by Western blot. *C*, HEK293T cells were transfected with plasmids expressing EGFP (vector control), SipC-EGFP, SipC-C-EGFP, and SipC-N-EGFP. The interaction in cell lysates between SipC and actin was examined by coimmunoprecipitation with anti-GFP antibodies followed by Western blot using anti-actin or GFP antibodies.

chromosome of *Salmonella* that are devoid of *sipAsopB* resulting in *sipAsopBsipC*#2 and *sipAsopBsipC*#3, respectfully. Mutation sipC#10 was eliminated from this experiment because it is deficient in all effector translocation (21). Mutation *sipC*#5 (active in F-actin bundling) was similarly introduced into the chromosome of *Salmonella sipAsopB* as a control. We first showed that the *sipAsopBsipC*#2, *sipAsopBsipC*#3, and *sipAsopBsipC*#5 mutant strains maintained their effector translocation activity similar to that of parent *sipAsopB* strain (data not shown). We then tested these strains for their ability to invade HeLa cells. The *sipAsopBsipC*#2 and *sipAsopBsipC*#3 mutant strains were significantly less invasive when compared with that of their parent *sipAsopB* strain (Fig. 5). The invasion defects were restored upon the introduction of a plasmid encoding the wild-type SipC into the *sipAsopBsipC*#2 and *sipAsopBsipC*#3 mutant strains (Fig. 5). Similar results were obtained in human Caco-2 cells (data not shown). These data demonstrate that the bundling-deficient *sipC* mutants had lower invasion rates than that of the wild-type SipC.

## DISCUSSION

Multifunctional proteins pose significant challenges to study because the traditional null mutation, knock-out, or knock-down strategies have limited use. Small mutations are often created to abolish one activity while maintaining other known activities. *Salmonella* SipC is known to have actin nucleation, F-actin bundling, and type III effector translocation activities. We have successfully used small deletion replacement mutagenesis approaches to create mutant SipC derivatives, which lose one of the mentioned activities. We presented data here indicating that the SipC C terminus (amino acids 381–409) contains the F-actin binding site. We further showed that amino acid residues 221–260 (#2 and #3) and 381–409 (#10) are required for the bundling activity in either the truncated SipC-C or the full-length SipC.

Previous studies have shown that SipC protein mediates F-actin bundling activity and have suggested that the N terminus of SipC protein is responsible for this activity while the C-terminal region facilitates the actin nucleation activity (21,

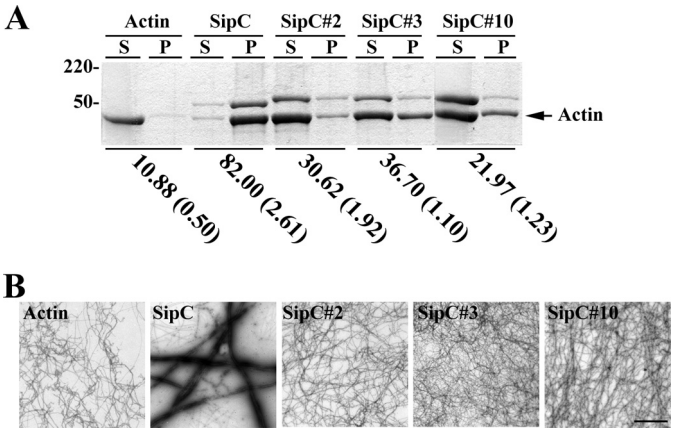


FIGURE 4. **The central (amino acids 221–260) and C-terminal (amino acids 381–409) regions of full-length SipC are involved in F-actin bundling.** *A*, F-actin bundling assay measured by the low speed co-sedimentation assay. F-actin was incubated alone, with full-length SipC or its full-length mutant derivatives at room temperature followed by centrifugation at 10,000 × *g* for 30 min. Supernatants and pellets were then resolved on an SDS-PAGE gel and visualized with Coomassie staining. The experiments were repeated five times and quantified by densitometry scanning. F-actin bundling activity was expressed as the percentage of actin that sediments in the total actin. Values represent means of five independent experiments with standard errors shown. *B*, F-actin bundles visualized by transmission election microscopy. F-actin was incubated alone, with full-length SipC or its full-length mutant derivatives.

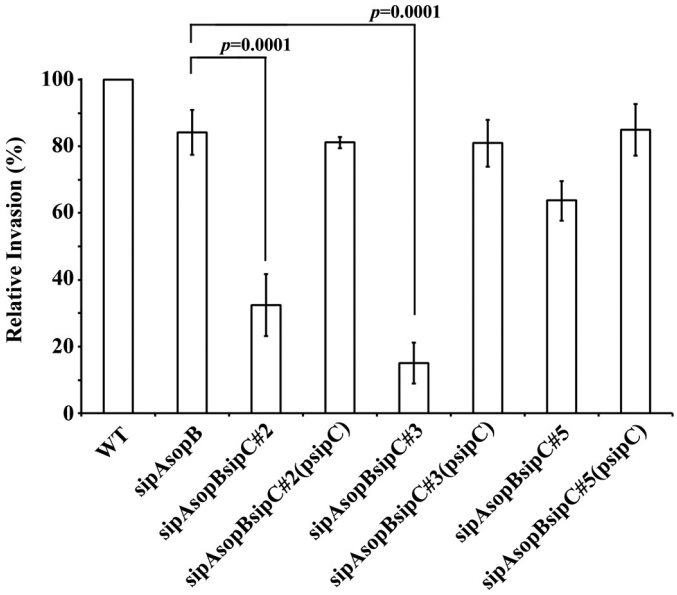


FIGURE 5. **SipC mutants deficient in F-actin bundling are less invasive into HeLa cells.** HeLa cells were infected with the wild-type *Salmonella* strain, *sipAsopB*-null mutant strain, *sipAsopBsipC*#2, *sipAsopBsipC*#3, *sipAsopBsipC*#5 mutant strains, or strains carrying plasmids expressing the corresponding mutant SipC proteins. The relative bacterial invasion was determined by the inside/outside differential staining assay. Data presented are from three independent experiments (>500 cells) with standard deviations shown. Statistical analysis was performed using Student's *t* test and GraphPad Prism 5 software.

27, 28). Data presented from this study demonstrate that the SipC C-terminal amino acid region (amino acids 200–409) possesses the F-actin bundling activity. We showed that both the truncated SipC-C and the full-length SipC possess F-actin bundling activity based on qualitative microscopy assay and the more quantitative co-sedimentation method. We further identified that amino acid residues 221–260 (#2 and #3) and 381–409 (#10) are required for the bundling activity using either the truncated SipC-C or the full-length SipC. Furthermore, we found that mutant strains deficient in F-actin bundling are less invasive into HeLa cells. These results indicate that the F-actin bundling activity of SipC plays a significant role during *Salmonella* infection.

As mentioned above, a previous report (28) showed that the N terminus of SipC had F-actin bundling activity while the C terminus did not. This is contrary to our data that the C terminus of SipC possesses the F-actin bundling activity. It is known that recombinant SipC proteins form inclusion bodies and often have to be purified under denaturing conditions. It is possible that some of the purified recombinant SipC proteins lost their actin bundling activities. Whereas there are no other known testable activities for the N terminus of SipC, it has been demonstrated that the nucleation and translocation activities lie within the C terminus of SipC (21, 28). Our purified recombinant SipC-C maintained its actin bundling activity levels comparable to that of the full-length wild-type SipC, indicating that the N terminus of SipC is dispensable for its bundling activity. In addition, our *in vitro* biochemical data showed that amino acid residues 221–260 (#2 and #3) and 381–409 (#10) were required for the actin bundling activity of SipC. Although full-length #2, #3, and #10 mutant SipC and the truncated SipC-C lost their bundling activities, their actin nucleation activities did not change. Furthermore, the chromosomal mutants *sipC*#2 and *sipC*#3 had comparable translocation activities to that of the wild-type *Salmonella*. Taken together, our data strongly support the conclusion that the C terminus of SipC has F-actin bundling activity.

The biochemical mechanism by which SipC mediates its F-actin bundling activity remains unclear. In general, F-actin bundling activity requires at least two independent F-actin binding sites or a combination of one binding site plus a self-association domain. We have shown previously that wild-type SipC is capable of forming dimers (27). It is tempting to speculate that SipC might self-associate to bundle F-actin filaments using its C-terminal F-actin binding site. Our preliminary data showed that mutant #2, 3, and #10 remain capable of forming dimers (data not shown). Because #2, #3, and #10 had lower F-actin binding activity, we speculate that the bundling defect is likely caused by the loss of binding to actin, rather than the inability to form dimers.

*Salmonella*-induced actin cytoskeleton rearrangements result from complex and combined action of multiple bacterial effectors and host proteins (7). It is well recognized that mutations in one type III effector often result in minor, transient, or even undetectable phenotypes in tissue-cultured cells. Cooperation between *Salmonella* SipA and SipC has been reported using *in vitro* biochemical assays (31). SipC has also been shown to synergize the activity of SipA, SopB, and SopE within cultured cells (32). We have shown previously that the actin nucleation-deficient SipC mutant #1 had reduced levels of actin cytoskeleton rearrangements in infected HeLa cells (21). We did not observe dramatic differences in cytoskeleton rearrangements in various tissue-culture cells when the chromosomal mutants *sipC*#2 and *sipC*#3 were used. When the *sipC*#2 and *sipC*#3 mutations were introduced into the chromosome of

*sipAsopB* mutant *Salmonella*, we found that the *sipAsopB-sipC*#2 and *sipAsopBsipC*#3 mutant strains were significantly less invasive when compared with that of their parent *sipAsopB* strain. These data demonstrate that the SipC F-actin bundling activity is important in *Salmonella* entry into host cells and likely exert its actin modulating activity in conjunction with SipA and SopB.

It is becoming evident that *Salmonella*-induced host actin cytoskeleton rearrangements result from the intricate interplay between numerous bacterial effector molecules and host cytoskeleton proteins. The bacterial effectors exploit the cytoskeleton at both the signaling pathways and at the actin dynamics by binding/interacting with components of the actin cytoskeleton directly. It is not known why *Salmonella* strains evolved the multi-functional SipC to affect the host actin cytoskeleton. It is possible that by having the translocation activity and actin modulating activity associated with the SipC protein, *Salmonella* strains are able to mount a more prominent, and yet localized, actin cytoskeleton rearrangements at the site of bacterial contact. Future studies will help us to understand how various activities are coordinated during *Salmonella* invasion.

## REFERENCES


1. Galán, J. E. (1999) *Curr. Opin. Microbiol.* **2,** 46–50
2. Galán, J. E., and Collmer, A. (1999) *Science* **284,** 1322–1328
3. Galán, J. E., and Curtiss, R., 3rd (1989) *Proc. Natl. Acad. Sci. U.S.A.* **86,** 6383–6387
4. Galán, J. E., and Wolf-Watz, H. (2006) *Nature* **444,** 567–573
5. Galán, J. E., and Zhou, D. (2000) *Proc. Natl. Acad. Sci. U.S.A.* **97,** 8754–8761
6. Kubori, T., Matsushima, Y., Nakamura, D., Uralil, J., Lara-Tejero, M., Sukhan, A., Galán, J. E., and Aizawa, S. I. (1998) *Science* **280,** 602–605
7. Zhou, D., and Galán, J. E. (2001) *Microbes Infect.* **3,** 1293–1298
8. Zhou, D., Mooseker, M. S., and Galán, J. E. (1999) *Science* **283,** 2092–2095
9. Hardt, W. D., Chen, L. M., Schuebel, K. E., Bustelo, X. R., and Galán, J. E. (1998) *Cell* **93,** 815–826
10. Fu, Y., and Galán, J. E. (1999) *Nature* **401,** 293–297
11. Zhou, D., Chen, L. M., Hernandez, L., Shears, S. B., and Galán, J. E. (2001) *Mol. Microbiol.* **39,** 248–259
12. Kaniga, K., Tucker, S., Trollinger, D., and Galán, J. E. (1995) *J. Bacteriol.* **177,** 3965–3971
13. Kaniga, K., Trollinger, D., and Galán, J. E. (1995) *J. Bacteriol.* **177,** 7078–7085
14. Hueck, C. J., Hantman, M. J., Bajaj, V., Johnston, C., Lee, C. A., and Miller, S. I. (1995) *Mol. Microbiol.* **18,** 479–490
15. Fu, Y., and Galán, J. E. (1998) *Mol. Microbiol.* **27,** 359–368
16. Miao, E. A., Scherer, C. A., Tsolis, R. M., Kingsley, R. A., Adams, L. G., Bäumler, A. J., and Miller, S. I. (1999) *Mol. Microbiol.* **34,** 850–864
17. Matsudaira, P., Mandelkow, E., Renner, W., Hesterberg, L. K., and Weber, K. (1983) *Nature* **301,** 209–214
18. de Arruda, M. V., Watson, S., Lin, C. S., Leavitt, J., and Matsudaira, P. (1990) *J. Cell Biol.* **111,** 1069–1079
19. Tsukita, S., Mimura, N., Tsukita, S., Khono, K., Ohtaki, T., Oshima, T., Ishikawa, H., and Asano, A. (1988) *Cell Motil. Cytoskeleton* **10,** 451–463
20. George, S. P., Wang, Y., Mathew, S., Srinivasan, K., and Khurana, S. (2007) *J. Biol. Chem.* **282,** 26528–26541
21. Chang, J., Chen, J., and Zhou, D. (2005) *Mol. Microbiol.* **55,** 1379–1389
22. Hoiseth, S. K., and Stocker, B. A. (1981) *Nature* **291,** 238–239
23. Kaniga, K., Delor, I., and Cornelis, G. R. (1991) *Gene* **109,** 137–141
24. Spudich, J. A., and Watt, S. (1971) *J. Biol. Chem.* **246,** 4866–4871
25. Yamagishi, A., Masuda, M., Ohki, T., Onishi, H., and Mochizuki, N. (2004) *J. Biol. Chem.* **279,** 14929–14936
26. Blanchoin, L., Amann, K. J., Higgs, H. N., Marchand, J. B., Kaiser, D. A., and Pollard, T. D. (2000) *Nature* **404,** 1007–1011
27. Chang, J., Myeni, S. K., Lin, T. L., Wu, C. C., Staiger, C. J., and Zhou, D. (2007) *Mol. Microbiol.* **66,** 1548–1556
28. Hayward, R. D., and Koronakis, V. (1999) *EMBO J.* **18,** 4926–4934
29. Obert, S., O'Connor, R. J., Schmid, S., and Hearing, P. (1994) *Mol. Cell Biol.* **14,** 1333–1346
30. Jepson, M. A., Kenny, B., and Leard, A. D. (2001) *Cell Microbiol.* **3,** 417–426
31. McGhie, E. J., Hayward, R. D., and Koronakis, V. (2001) *EMBO J.* **20,** 2131–2139
32. Cain, R. J., Hayward, R. D., and Koronakis, V. (2008) *PLoS Pathog.* **4,** e1000037